

Expression pattern of histone lysine-specific demethylase 6B in gastric cancer

SHUJUN WANG*, YIPING WANG*, HUI ZHU, MIAOHUI CHEN and LIANG ZHANG

Department of Gastroenterology, Cixi People's Hospital, Affiliated Cixi Hospital,
Wenzhou Medical University, Cixi, Zhejiang 315300, P.R. China

Received March 7, 2020; Accepted March 17, 2021

DOI: 10.3892/ol.2021.12752

Abstract. Over the last few decades, predictive markers for the prognosis of gastric cancer have not been extensively investigated. The present study aimed to evaluate the expression profile of histone demethylase lysine (K)-specific demethylase 6B (KDM6B) in gastric cancer and healthy control tissues, as well as its value in prognosis prediction as a clinical marker. Within the framework of these criteria, the diagnostic role of KDM6B for gastric cancer was investigated, which may provide insights into novel treatment targets. Immunohistochemistry was applied to detect KDM6B expression in 100 gastric cancer tissues and matching para-cancerous tissues to analyze the association between KDM6B expression and clinicopathological features. Based on the follow-up data, the value of KDM6B in prognosis assessment was further explored. The role of KDM6B in gastric cancer cell proliferation, cell cycle distribution and the expression of cell cycle-associated proteins was investigated by inhibiting KDM6B activity using the specific inhibitor GSK J4. KDM6B was mostly distributed in cytoplasm and nucleus in gastric cancer tissue. The expression level was significantly higher in cancer tissues compared with that in the corresponding non-cancerous tissues. The expression of KDM6B was significantly associated with sex, lymph node and distant metastasis status and clinical stage ($P < 0.05$). Cell proliferation was significantly decreased with the inhibition of KDM6B activity, and the cell cycle in HGC27 cells was arrested in the G₂/M phase after being treated with GSK J4 for 24 h. The expression of cyclin B and Cdc2 were significantly decreased, while p21 was upregulated. It was concluded that the dysregulated expression of KDM6B is associated with the

malignant progression of gastric cancer and could be a potential marker for prognosis. Blocking the demethylase activity of KDM6B induced G₂/M arrest and inhibited the proliferation of gastric cancer cells, suggesting that KDM6B is a potential novel therapeutic target for gastric cancer.

Introduction

It has been reported that gastric cancer is the fifth most frequent malignancy worldwide and almost one million new cases are estimated to occur each year, resulting in ~723,000 deaths per year globally (1,2). In >50% of cases, gastric cancer has no noticeable symptoms, which may lead to advanced carcinoma with multiple metastases upon diagnosis (3). Chemotherapy is still considered as the primary therapy for advanced gastric cancer; however, its disadvantages, such as low response rate and short duration of clinical benefit, have limited its application (4). It is important to identify and develop more specific targeted therapies to improve the prognosis of gastric cancer. To achieve this, it is essential to screen and identify the critical molecular pathways and signaling transduction networks involved in the pathogenesis of gastric cancer using in-depth studies.

In 2017, Padmanabhan *et al* (5) reported that epigenetic dysregulation plays an essential role in the development of gastric cancer. Post-translational histone modifications are involved in the malignant progression of gastric cancer by regulating the expression of oncogene and tumor suppressor genes. The occurrence of gastric cancer is a result of the combination of environmental, polygenic and epigenetic abnormalities. The epigenetic mechanisms involved include DNA methylation (6), non-coding RNA (7) and histone translational modifications (8). Among these regulations, histone modifications, such as acetylation (9), methylation (10) and ubiquitination (11), are involved in the carcinogenesis of gastric mucosa through the regulation of oncogene expression (12) and protein-protein interactions (13). For example, while a group of genes including phosphatidylserine decarboxylase proenzyme, SWI/SNF complex subunit SMARCC1 and vacuolar protein sorting-associated protein 37A are aberrantly methylated, thus aberrantly expressed, in gastric cancer (12), antisense-transcribed lncRNA HOXA11-AS is upregulated and serves as a scaffold to form complex of chromatin modification factors polycomb repressive complex 2, lysine-specific histone

Correspondence to: Dr Shujun Wang, Department of Gastroenterology, Cixi People's Hospital, Affiliated Cixi Hospital, Wenzhou Medical University, 999 East Road of South 2nd Ring, Cixi, Zhejiang 315300, P.R. China
E-mail: wshujun@yahoo.com

*Contributed equally

Key words: gastric cancer, lysine (K)-specific demethylase 6B, expression profiles, prognosis, GSK J4, G₂/M arrest

demethylase 1A and DNA (cytosine-5)-methyltransferase 1, thus regulating downstream gene expression, including prostaticin and Krueppel-like factor 2 (13).

Post-translational histone modifications are involved in the malignant progression of gastric cancer by regulating the expression of oncogene and tumor suppressor genes. For instance, hypermethylation of histone 3 at lysine 9, hypomethylation of histone 3 at lysine 4 and hypoacetylation of histone 3 at lysine 9 are reported to be associated with the silencing of tumor suppressor genes P16 and *mutL* homolog 1 (MLH1) in gastric cancer cells (14). Moreover, the aberrant expression of an oncogene, Fez family zinc finger protein 1, is highly regulated by DNA methylation and histone acetylation in gastric cancers (15). Histone methylation modification is an essential regulatory mechanism in chromatin structure alteration and gene transcription (16). As a member of the histone demethylase family of proteins containing a JmjC domain, lysine (K)-specific demethylase 6B (KDM6B) reverses the dimethylation (H3K27me2) and trimethylation (H3K27me3) of lysine at the 27th position in histone H3 and then activates the expression of target genes, such as proinflammatory factors including the p19 peptide of the chimeric cytokine IL-23, granulocyte colony-stimulating factor and triggering receptor expressed on myeloid cells 1 (17). The overexpression of KMD6B is found in numerous types of tumor, such as prostate cancer, diffuse large B cell lymphoma and renal clear cell carcinoma, and it is associated with tumor progression and poor prognosis (18-20).

The present study analyzed the expression profile of KMD6B in gastric cancer and further explored the functions and the potential underlying mechanisms of KDM6B in gastric cancer development. Furthermore, the alterations in cell proliferation, cycle distribution and the expression of cell cycle related proteins after inhibiting KMD6B with its specific inhibitor GSK J4 were investigated. The present study reported novel evidence to support the association between KMD6B-overexpression and gastric cancer and evaluated KMD6B as a possible risk factor for gastric cancer.

Materials and methods

Patients and ethics approval. In total, 100 adult patients with cancer were admitted to Cixi People's Hospital between March 2008 and December 2011. Patients with gastric cancer who underwent surgical resection or gastroscopic biopsy were included in the present study. The age range was from 32 to 81 years old, with the median age of 65 years. Each case was diagnosed according to the World Health Organization classification of digestive system tumors (2010 edition) (21) by two pathologists who were blinded to patients' identification and followed up every six months in clinic until December 2018. The detailed flow chart of the present study is presented in Fig. 1. All patients were newly diagnosed, without radiotherapy and chemotherapy or other tumor histories. No other inclusion or exclusion criteria were applied. The selected adjacent non-cancerous tissues were at ≥ 2 -cm away from the edge of the cancer tissue. Tissues were fixed in 10% neutral formalin, processed through the standard dehydration and paraffin embedding protocol. Briefly, tissues were fixed in 10% neutral formalin for 24 h at 4°C, followed by dehydrating

in 70% ethanol, two changes, 1 h each; 80% ethanol, one change, 1 h; 95% ethanol, one change, 1 h; 100% ethanol, three changes, 1.5 h each; and xylene, three changes, 1.5 h each. Then the tissues were embedded in paraffin. Written informed consent for the use of medical records of the patients was obtained at the time of surgery. The study was approved by The Ethics Committee of Cixi Hospital (Cixi, China; approval nos. 2008-005 and 2017-LS-25).

Cells and reagents. The human gastric cancer cell line HGC-27 was purchased from The Cell Bank of Type Culture Collection of the Chinese Academy of Sciences and cultured in RPMI-1640 medium with 10% fetal bovine serum (both Thermo Fisher Scientific, Inc.). KMD6B inhibitor GSK J4 was purchased from Selleckchem (purity $\geq 98\%$); rabbit anti-human KMD6B, cyclin B1, Cdc2, p21 and GAPDH polyclonal antibodies and horseradish peroxidase enzyme (HRP)-labeled goat anti-rabbit IgG antibodies were purchased from Cell Signaling Technology, Inc.

Immunohistochemistry (IHC) and hematoxylin-eosin (HE) staining. IHC and HE staining were performed using the Histostain™ kit (Thermo Fisher Scientific, Inc.) following manufacturer's protocol. Briefly, paraffin embedded samples were sectioned into 5- μ m sections. Tissue slides were deparaffinized and rehydrated by immersing the slides through the following solutions: Xylene (three washes 5 min each) 100, 95, 70 and 50% ethanol (each washed twice for 10 min each) and deionized water, two washes for 5 min each. The slides were then fixed in 10% paraformaldehyde for 10 min at room temperature and washed with PBS. Fixed samples were treated with 3% H₂O₂ solution at room temperature for 10 min followed by washing with PBS three times. Antigen retrieval was performed by soaking the slides in boiling 0.01 M citrate buffer, pH 6.0 for 10 min, cooling to room temperature and washing with PBS three times. Tissue sections were incubated with serum blocking solution provided in the kit for 10 min, followed by incubation with rabbit primary antibody against KMD6B (cat. no. EAB-2167; 1:50; Abcam) at room temperature for 1 h. After washing with PBS, sections were incubated with biotinylated broad-spectrum secondary antibody (Histostain®-Plus 3rd Gen IHC Detection Kit, Invitrogen, #85-903) at room temperature for 10 min and washed with PBS as the manufacture suggested. After incubation, sections were then incubated with streptavidin-enzyme conjugate for 10 min at room temperature, washed with PBS and incubated with substrate-chromogen mixture at room temperature for 5 min, washed with PBS again and counterstained with hematoxylin for 1 min at room temperature following by thorough rinsing with tap water. Sections were finally mounted and dried until observation. Images were captured using a pathology microscopy imaging system (Olympus Corporation). Qualitative staining refers yellowish to brownish yellow staining as a positive marker in sections and sections were divided into four categories depending on staining intensity: 0, clear, 1, weak, 2, moderate and 3, strong. Colored areas were 0, if positive cells percentage $\leq 1\%$; 1, $>1\%$ to $\leq 25\%$; 2, $>25\%$ to $\leq 50\%$ and 3, $>50\%$. If the sum of the intensity score and the positive percentage score was >3 , it was considered as high expression of KMD6B.

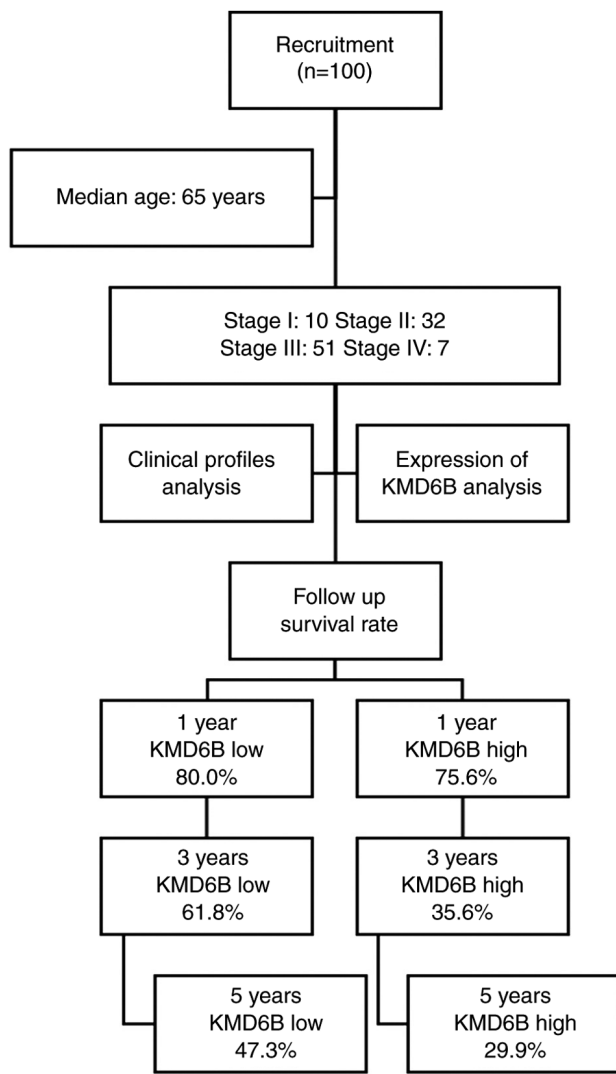


Figure 1. Study flow chart. KMD6B, lysine (K)-specific demethylase 6B.

In vitro proliferation analysis. The viability of HGC-27 cells was determined by staining the cells with trypan blue following the manufacturer's instructions (Thermo Fisher Scientific, Inc.). The cells were treated with either vehicle control (0 μM) or GSK J4 at 2 or 4 μM for 24, 48 and 72 h. After treatment, cells were trypsinized and resuspended in culture medium and then counted under the microscope. For the colony formation assay, HGC27 cells were seeded in six-well plate with 1×10^4 cells per well. GSK J4 was added into the culture medium at the concentrations of 0, 2 and 4 μM . Cell culture medium with appropriate concentration of GSK J4 were refreshed every other day during the treatment. After 7 days incubation at 37°C, the cells were fixed with 4% paraformaldehyde solution for 10 min at room temperature and stained by 0.1% crystallization purple for 15 min at 37°C. The formation of colonies was analyzed (five fields randomly selected for counting clones, which is defined as a colony ≥ 10 cells). For cell cycle analysis, cells were trypsinized after treatment and were fixed with 100% ethanol at -20°C for 10 min, followed by washing with TBS at room temperature and rehydrating in PBS for 10 min. Cells were then stained with propidium iodide (PI) at 1 $\mu\text{g/ml}$ (BioLegend, Inc.). Flow cytometry

(BD FACSLyric™ Research System; BD Biosciences, Inc.) was used to run the samples and the data were analyzed using the ModFitLT software (ModFit5.0™; VeritySoftwareHouse, Inc.). In the meantime, the PrestoBlue® Cell Viability Reagent (Thermo Fisher Scientific, Inc.) was employed for the cell viability and proliferation detection. Briefly, 10 μl PrestoBlue reagent was added to 90 μl culture media at 37°C in a cell culture incubator, protected from direct light for 30 min. Next, 100 μl media collected from the culture wells was used for absorbance quantification at 570 nm, using 600 nm as a reference wavelength, using a plate reader.

Western blotting. Cell culture and drug treatment were performed as aforementioned. Total cell lysate was extracted with RIPA buffer (Thermo Fisher Scientific, Inc.), and the protein concentration was determined using the BCA method. Then samples were analyzed by using 12% SDS-PAGE with 20 μg loaded per lane. Then the proteins were transferred to PVDF membranes at 300 mA constant current for 120 min. The membrane was blocked with 3% BSA for 1 h at room temperature, then incubated with anti-cyclin B1 (cat. no. 12231; Cell Signaling Technology Inc.), Cdc2 (cat. no. 28439; Cell Signaling Technology, Inc.) and p21 (Cell Signaling Technology Inc.). All the primary antibodies used were diluted at 1:1,000. for 2 h at room temperature, washed with TBS-T (0.1% Tween-20 in TBS) for 10 min three times. Then the membranes were incubated with HRP-labeled goat anti-rabbit IgG secondary antibody at room temperature for 1 h and washed with TBST. The Pierce™ ECL Western Blotting Substrate reagent (Thermo Fisher Scientific, Inc.) was used to visualize following the manufacturer's instructions. GAPDH was used as the internal control.

Statistical analysis. GraphPad Prism 8 (GraphPad Software, Inc.) was used for data analysis. All data sets were tested for the normal distribution. The χ^2 test was used to compare the data over the expressions or profiles (such as tissue origin, expression level, age or sex). Fisher's exact tests were also used where appropriate. Cox univariate analysis was performed to analyze prognostic factors in patients as a whole. Cox multivariate analysis was performed to analyze prognostic factors in male vs. female patients. Clinical survival data was analyzed using Kaplan-Meier analysis with the log-rank test performed. *In vitro* experiment times was represented in each figure legends. Data sets were analyzed with one-way ANOVA followed by Tukey's or Dunnett's post hoc tests as appropriate. $P < 0.05$ was considered to indicate a statistically significant difference.

Results

Expression of KMD6B in gastric cancer tissues and the matching para-cancerous tissues. In total, 100 adult patients were included in the present study, including 10 stage I, 32 stage II, 51 stage III and seven stage IV. To investigate whether the gastric cancer had increased KMD6B expression compared with para-cancerous tissue, IHC and HE staining and analysis were performed. There were 45 cases of KMD6B high expression among 100 cases of gastric cancer tissues, which accounted for 45.0% of the tested samples,

Table I. Expression of KMD6B in gastric cancer tissues and the matched para-cancerous tissues.

Tissue origin	Value, n	KMD6B expression, n (%)		P-value
		High	Low	
Cancer tissue	100	45 (45)	55 (55)	0.028 ^a
Para-cancerous tissue	100	30 (30)	70 (70)	

^aP<0.05. KMD6B, lysine (K)-specific demethylase 6B.

seeing a significant difference compared with 30 cases among adjacent para-cancerous tissues, with the positive rate of 30.0% (P=0.028; Table I) (Fig. 2).

Relationship between KMD6B expression in gastric cancer and clinical profiles. Next, whether the overexpression of KMD6B had any correlation with the clinical characteristics was investigated. Demographic and clinical characteristics were analyzed, as shown in Table II. KMD6B expression was not associated with patient age, tumor size, location, degree of differentiation, nerve and vascular invasion and T stage, with the corresponding P-values, 0.917, 0.393, 0.611, 0.270, 0.685 and 0.191, respectively. The expression of KMD6B was associated with sex, N, M and clinical stages, with P-values of 0.029, 0.020, 0.021 and 0.021, respectively.

KMD6B expression may serve as gastric cancer prognostic factor. To investigate whether KMD6B has the potential to predict patient prognosis, expression levels of KMD6B and patient mortality rate were analyzed. In 45 cases that were considered as KMD6B high expression, the 1-, 3- and 5-year cumulative survival rates were 75.6, 35.6 and 29.9%, respectively. Whereas in the 55 cases with KMD6B low expression, the 1-, 3- and 5-year cumulative survival rates were 80.0, 61.8 and 47.3%, respectively (Fig. 1). The overall survival rate of patients with KMD6B low expression was significantly higher compared with that of the high expression group (P=0.020) (Fig. 3). These data indicated that the expression of KMD6B might have the potential to serve as a prognostic biomarker for gastric cancer.

A total of 11 other variables were also analyzed, including age, sex, tumor size, tumor location, differentiation degree, nerve/vascular invasion, T, N, M and clinical stage and KMD6B expression level. As shown in Table III, Cox univariate analysis suggested that nine out of 11 variables could serve as prognostic factors, including age (P=0.023), tumor size (P=0.013), degree of differentiation (P=0.017), neurovascular invasion (P<0.001), T stage (P=0.016), N stage (P=0.021), M stage (P<0.001), clinical stage (P=0.031) and KMD6B expression level (P=0.023).

Multivariate analysis reported eight significant independent predictors, including age, sex, tumor size, tumor location, the degree of differentiation, nerve/vascular invasion, clinical stage and KMD6B expression. The results demonstrated that tumor size (P=0.008), neurovascular invasion (P<0.001) and

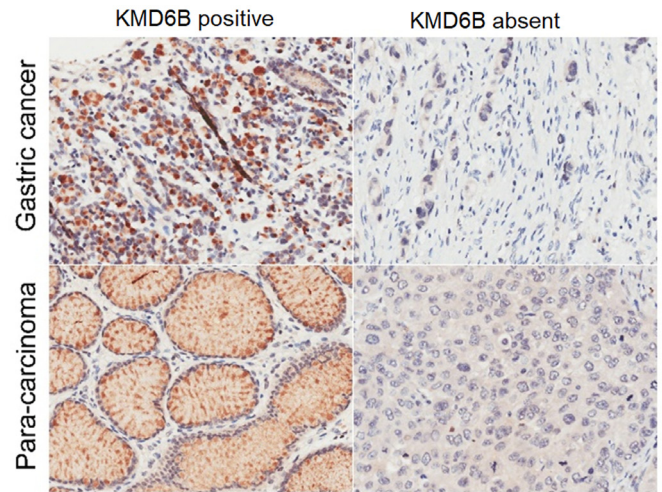


Figure 2. Expression of KMD6B in gastric cancer tissues and matched para-carcinoma tissues (magnification, x200). KMD6B, lysine (K)-specific demethylase 6B.

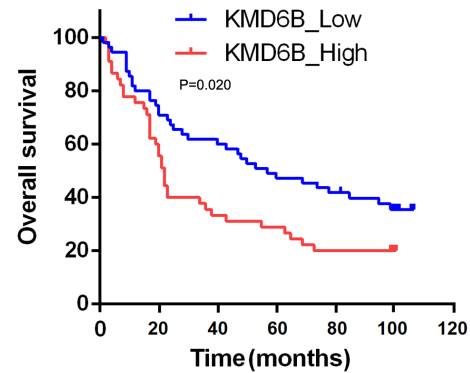


Figure 3. Comparison of the Kaplan-Meier survival curves on different expression levels of KMD6B in tumor cells of patients with gastric cancer. KMD6B, lysine (K)-specific demethylase 6B.

KMD6B expression (P=0.007) were independent prognostic predictors of gastric cancer (Table IV).

GSK J4 inhibits the proliferation of gastric cancer HGC27 cells. The aforementioned data indicated that expression pattern of KMD6B could serve as an independent prognostic factor in gastric cancer. Due to its significantly upregulated expression in gastric cancer tissues, it was speculated if overexpression also contributes to the malignant development of gastric mucosa. Cell proliferation was assessed by specific inhibition by GSK J4. The gastric cancer cell line HGC27 was used to perform a proliferation assay with 3 days of GSK J4 treatment. The density of HGC27 cells in GSK J4 group was significantly less compared with that in the control group (P<0.05; Fig. 4). After 24-h treatment, cells showed different proliferation rates. In vehicle control group, cell number reached $2.5 \pm 0.4 \times 10^5$, which was almost doubled that of the starting cell numbers ($1.8 \pm 0.1 \times 10^5$), whereas in GSK J4-treated cells, both drug concentrations used inhibited cell proliferation. The difference became more evident with increasing doses. As shown in Fig. 4B, by the end of treatment, the number of cells treated with GSK J4 $4 \mu\text{M}$ was ~4-fold less compared with the

Table II. Association between KMD6B expression in gastric cancer and clinical profiles.

Clinical variable	Value, n	KMD6B expression, n		P-value
		High	Low	
Age, years				0.917
<65	45	20	25	
≥65	53	23	30	
Sex				0.029 ^a
Male	64	34	30	
Female	36	11	25	
Tumor size, cm				0.393
<5	51	25	26	
≥5	47	19	28	
Tumor location				0.611
Cardia/fundus	13	5	8	
Body/antrum	87	40	47	
Pathological grade				0.270
I	37	14	23	
II/III	63	31	32	
Nerve/vessel invasion				0.685
No	86	38	48	
Yes	14	7	7	
T stage				0.191
1/2	19	6	13	
3/4	81	39	42	
N stage				0.020 ^a
0	27	7	20	
1-3	73	38	35	
M stage				0.021 ^a
0	92	38	54	
1	8	7	1	
Clinical stage				0.021 ^a
I	10	1	9	
II/III/IV	90	44	46	

^aP<0.05. KMD6B, lysine (K)-specific demethylase 6B.

vehicle treated group (7.6 ± 0.4 vs. 1.9 ± 0.2 ; $P < 0.05$). GSK J4 $2 \mu\text{M}$ treatment also showed the significant inhibitory function compared with the control group (2.2 ± 0.1 vs. 1.9 ± 0.2 ; $P < 0.05$).

GSK J4 inhibits the colony formation of gastric cancer cells. A colony formation assay was also used to test the inhibitory effect of GSK J4 on gastric cancer cells. Following treatment with GSK J4 for 7 days, the colony number was 37.3 ± 15.5 and 16.0 ± 5.6 in GSK J4 ($2 \mu\text{M}$) and GSK J4 ($4 \mu\text{M}$) groups, respectively. However, there were 179.0 ± 13.5 colonies in the control group, suggesting that GSK J4 can inhibit the proliferation of gastric cancer cells. Compared with the traditional the formation of colonies, the resazurin-based PrestoBlue

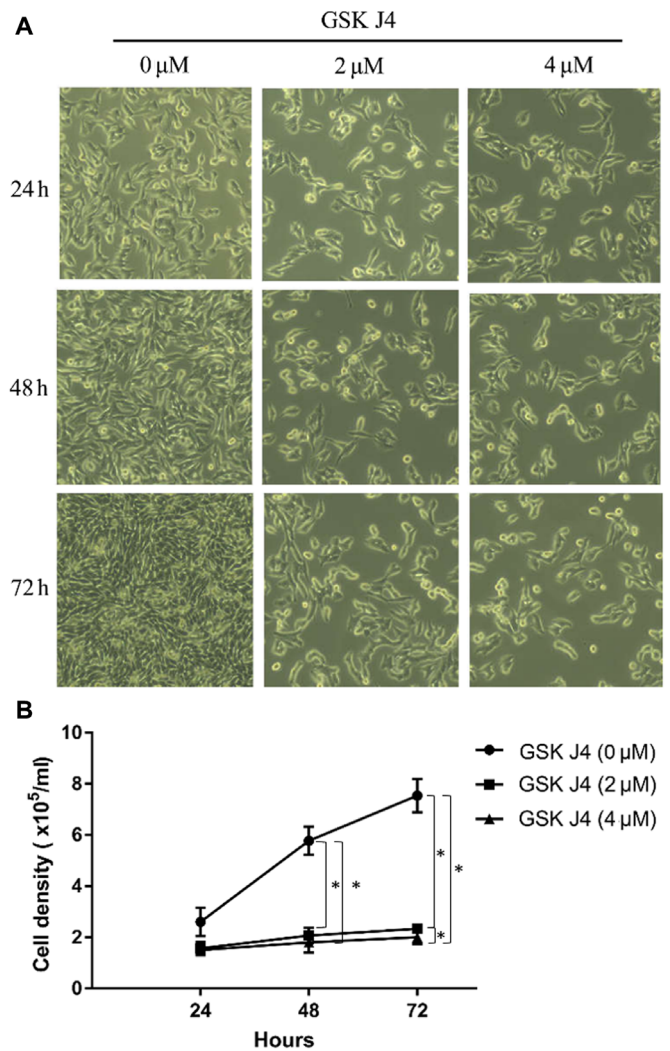


Figure 4. KMD6B regulates cell proliferation through demethylation. (A) Proliferation of gastric cancer cells was inhibited by blocking the demethylase activity of KMD6B. (B) Cell counting after blocking KMD6B activity. ^aP<0.05 vs. control or GSK J4 $4 \mu\text{M}$. KMD6B, lysine (K)-specific demethylase 6B.

cell viability assay represented the similar results, with significant inhibition of cell proliferation between the GSK J4 2 and $4 \mu\text{M}$ groups compared with the vehicle-treated group (0.887 ± 0.088 vs. 1.810 ± 0.206 , $P = 0.0049$, and $0.0.623 \pm 0.055$ vs. 1.810 ± 0.206 , $P = 0.0013$, respectively; Fig. 5).

Effects of GSK J4 on cell cycle distribution and related protein expression of gastric cancer cells. Next, it was investigated how GSK J4 inhibited gastric cancer cell proliferation. Flow cytometry was used to analyze the cell cycle progression of cells treated with GSK J4. Following treatment with GSK J4 2 and $4 \mu\text{M}$ for 24 h, the percentage of HGC27 cells at G₂ phase were 35.76 ± 2.40 and $41.62 \pm 9.47\%$ respectively, which was significantly increased compared with the control group ($18.80 \pm 2.05\%$) (both $P < 0.05$). In the G₁ or S phase, the percentage of HGC27 cells after GSK J4 treatment showed the trends of inhibition, compared with the control group but no significant difference been observed (Fig. 6). This suggested that blocking the demethylase activity of KMD6B can arrest the cell cycle at G₂/M phase.

Table III. Cox univariate analysis of prognostic factors of gastric cancer.

Variables	HR	LCI	UCI	P-value
Age, years, <65 vs. ≥65	0.580	0.363	0.927	0.023 ^a
Sex, female vs. male	0.614	0.378	0.997	0.048 ^a
Tumor size, cm, <5 vs. ≥ 5	0.551	0.344	0.883	0.013 ^a
Tumor location, cardia/fundus vs. body/antrum	1.465	0.727	2.956	0.286
Pathological grade, I vs. II/III	0.530	0.315	0.892	0.017 ^a
Nerve/vessel invasion, no vs. yes)	0.323	0.177	0.587	<0.001 ^b
T stage, 1/2 vs. 3/4	0.422	0.209	0.852	0.016 ^a
N stage, 0 vs. 1/2/3	0.510	0.288	0.903	0.021 ^a
M stage, 0 vs. 1	0.166	0.076	0.362	<0.001 ^b
Clinical stage, I vs. II/III/IV	0.280	0.088	0.892	0.031 ^a
KMD6B expression, low vs. high	0.580	0.363	0.927	0.023 ^a

^aP<0.05, ^bP<0.01. HR, hazard ratio; LCI, lower confidence interval; UCI, upper confidence interval.

Table IV. Multivariate Cox analysis of prognostic factors of gastric cancer, male vs. female.

Variable	Males			Females			P-value
	HR	LCI	UCI	HR	LCI	UCI	
Age, years, <65 vs. ≥65	0.631	0.385	1.249	0.711	0.429	0.965	0.118
Tumor size, cm, < 5 vs. ≥ 5	0.514	0.298	0.979	0.446	0.260	0.673	0.008 ^a
Tumor location, cardia/fundus vs. body/antrum	1.842	0.895	4.577	2.078	0.967	3.671	0.076
Pathological grade, I vs. II/III	0.818	0.521	1.475	0.762	0.383	1.291	0.410
Nerve/vessel invasion, no vs. yes	0.401	0.187	0.722	0.253	0.165	0.496	<0.001 ^a
Clinical stage, I vs. II/III/IV	0.629	0.210	1.802	0.515	0.130	2.056	0.368
KMD6B expression, low vs. high	0.501	0.288	0.741	0.419	0.234	0.879	0.007 ^a

^aP<0.01. HR, hazard ratio; LCI, lower confidence interval; UCI, upper confidence interval.

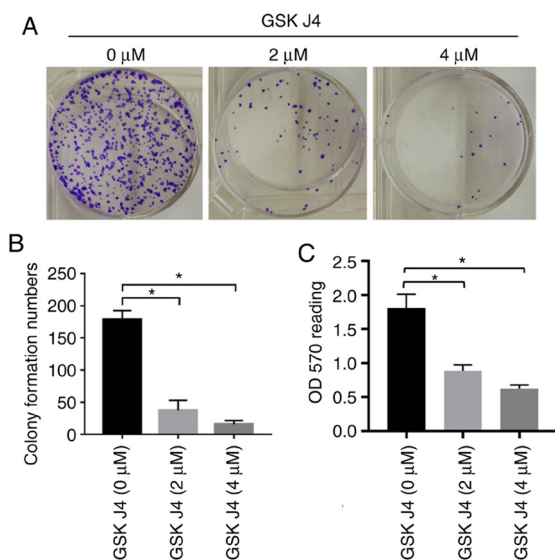


Figure 5. Colony formation of gastric cancer cells inhibited by blocking the demethylase activity of KMD6B. (A) Representative images of the colony formation assay. (B) Quantification of colony counting after blocking KMD6B. (C) Resazurin-based PrestoBlue[®] cell viability following GSK J4 2 and 4 μM treatment. *P<0.05 vs. control. KMD6B, lysine (K)-specific demethylase 6B.

Cell cycle is restrictedly regulated by a set of cell cycle regulating proteins. The expression level of those proteins is closely related to the cell cycle status (22). Western blotting was performed to analyze the expression level of key proteins involved in cell cycle. As shown in Fig. 7A and B, after 24-h treatment of GSK J4, the expression of cyclin B1 and Cdc2 in HGC27 cells was significantly downregulated (both P<0.05) while p21 was significantly upregulated compared with the control group (P<0.05).

Discussion

In China, the morbidity and mortality of gastric cancer are the third highest among all malignant tumors (2), of which >70% of patients are diagnosed at the advanced stage (3). Chemotherapy is the primary therapy for advanced gastric cancer even though the response rate is low and the duration of progression-free survival is short (4). Research has shown that different causes, including environmental causes and genetic abnormalities, contribute to the malignant transformation of gastric mucosa leading to gastric cancer progression (6-10). Among these genetic modifications, malfunction in epigenetic

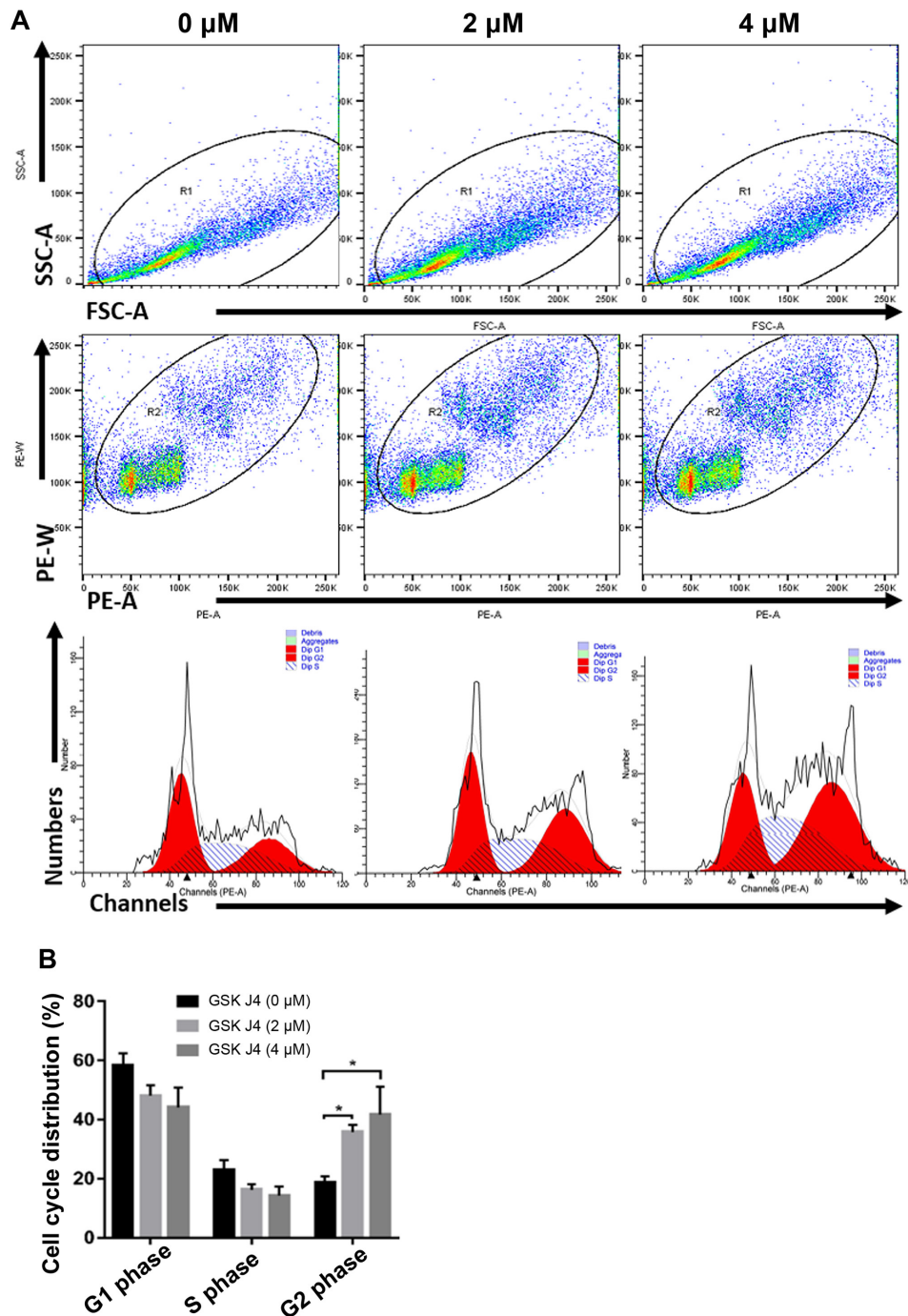


Figure 6. G₂/M phase arrest of gastric cancer cells induced by GSK J4 blocking the demethylase activity of lysine (K)-specific demethylase 6B. (A) Flow cytometry dot plots and histogram analysis represent the cells FSC/SSC and cell phases after GSK J4 treatment. (B) Cell cycle distribution after GSK J4 treatment. *P<0.05 vs. control. FSC, forward scatter; SSC, side scatter.

regulation of oncogenes or tumor suppressor genes is an area of interest, especially histone modifications including acetylation, methylation and ubiquitination. Epigenetic changes are involved in cancer progression by dysregulation of gene expression and/or protein-protein interaction (9-13). Intensive study of the pathogenesis of gastric cancer and screening key molecules involved in epigenetic regulation in gastric cancer will contribute to the development of targeted drugs and may improve the prognosis of patients with gastric cancer.

KMD6B is a member of the histone demethylase family of proteins containing the JmjC domain and requires Fe²⁺ and

α -ketoglutarate as co-factors (23). KMD6B alters the expression of target genes, such as those genes that are bivalently marked by H3K4me3 (tri-methylation at the 4th lysine residue of the histone H3) and H3K27me3 (tri-methylation at the 27th lysine residue of the histone H3) and associated with promoter-proximal, paused RNA polymerase II (24), to induce cell carcinogenesis by affecting the process of modifying factors binding and chromatin remodeling (1). KMD6B also directly regulates gene transcription by modifying H3K27 methylation in the promoter region of the Ink4a/Arf locus, which encodes two distinct proteins that intimately link the pRB and p53

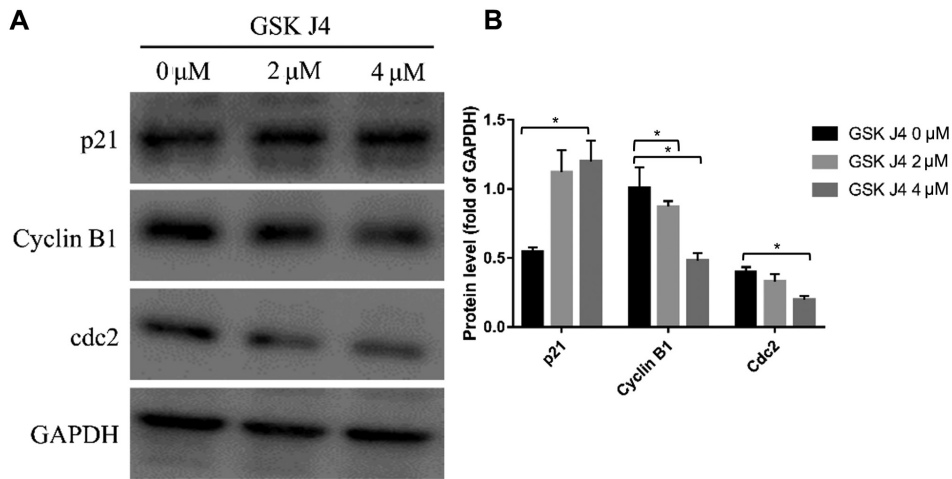


Figure 7. Cell cycle protein expression pattern upon GSK J4 treatment gastric cancer cells. (A) GSK J4 inhibited the expression of cyclin B1 and Cdc2 in gastric cancer cells but promoted p21 expression. (B) Quantification of western blotting. * $P < 0.05$ vs. GSK J4 0 or 4 μM group.

tumor suppressor pathways: p16INK4a and p14/p19ARF (25). KMD6B is overexpressed in different types of tumors and is associated with tumor progression and poor prognosis (26). KMD6B is upregulated in prostate cancer and expressed at the highest level in metastatic foci, and high KMD6B expression suggests a poor prognosis (19). KMD6B is also overexpressed in both primary and Epstein-Barr infection-related Hodgkin's lymphoma (27). Patients with renal clear cell carcinoma with KMD6B high expression have a poor prognosis, and the expression of KMD6B is positively correlated with the tumor size, lymph node metastasis and pathological stage (18). The present results indicated that KMD6B was highly expressed in 45% of gastric cancer tissues. The protein level of KMD6B was significantly associated with patient sex, N, M and clinical stages. Survival analysis showed that KMD6B-overexpression was an independent prognostic factor for gastric cancer. However, the sample distribution among clinical stage was unbalanced (I to II/III/IV, 1:9) in the study, which might be the reason why clinical stage cannot be used as a prognostic marker in gastric cancer in the present study. More patients with stage 1 are needed in order to analyze the relationship between clinical phases and gastric cancer prognosis. Similarly, the sex disproportion (male to female, 16:9) might affect the relationship between KMD6B expression and sex as well. Therefore, these factors require further study with a larger sample size. Such are expected to further demonstrate the impact of KMD6B on gastric cancer.

Targeted inhibition of the expression or demethylase activity of KMD6B can induce cell cycle arrest, apoptosis and differentiation, demonstrating the potent antitumor activity of KMD6B (22,28-30). GSK J4 inhibits KMD6B activity and decreases the self-renewal of breast cancer stem cells by downregulating the expression of the key transcription factors OCT4, NANOG and SOX2 (31,32). Ha *et al* (33) reported that KMD6B can promote G₁/S phase arrest in THP-1 cells. KMD6B mediates the malignant progression of diffuse large B cell lymphoma by sustaining the activation of the NF- κ B pathway via interacting with the transcription factor IRF4 and also can promote apoptosis resistance and cell proliferation (22,34,35). The present study demonstrated that GSK J4

significantly inhibited the proliferation of HGC27 gastric cancer cells as the percent of cells in the G₂ phase was increased in GSK J4-treated groups, the expression of cyclin B1 and Cdc2 was significantly decreased and p21 was upregulated.

The aforementioned experimental results suggested that the inhibition of endogenous KMD6B demethylase activity can induce G₂/M arrest and inhibit cell proliferation, suggesting KMD6B has potential as a therapeutic target for gastric cancer. Previous studies have found that KMD6B can promote the invasion and metastasis of hepatocellular carcinoma via mediating the epithelial-mesenchymal transition (EMT) through upregulating the expression of Slug (36,37). The present study has limitations, for example the database was extracted from single center and more cases are needed to validate the results. Moreover, clinical outcomes associated with cancer-wide gene expression and web-based platforms offering survival prediction data and cancer registry risk estimates, such as SurvExpress (38), PROGgeneV2 (39), UALCAN (www.ualcan.path.uab.edu) and Oncomine (www.oncomine.org), should be used in future. Using advanced genomic analysis tools could further improve our understanding of the impact of aberrant KMD6B on the clinical outcomes of gastric cancer (38-45). Since metastasis is a key malignant characteristic of cancer, it remains of considerable interest to further study the role of KMD6B in mediating the EMT phenotype. In addition, the potential of KMD6B targeted inhibition in preventing the invasion and metastasis of gastric cancer should be investigated.

Acknowledgements

Not applicable.

Funding

The study was funded by The Fund Project Science and Technology Plan Project of Cixi (grant no. CN2016023), The Medical, Health Science and Technology Program of Zhejiang Province (grant no. 2017KYB608) and The Traditional Chinese Medicine Research Fund of Zhejiang Province (grant no. 2018ZA119).

Availability of data and materials

The datasets used and/or analyzed during the present study are available from the corresponding author on reasonable request.

Authors' contributions

SW and YW conceived the present study. SW, YW, HZ, MC and LZ designed and performed the experiments. YW, HZ, MC and LZ analyzed and interpreted the data. SW and YW contributed to writing the manuscript. SW and YW confirm the authenticity of all the raw data. All authors read and approved the final version of the manuscript.

Ethics approval and consent to participate

The study complied with the standards of the Declaration of Helsinki and was approved by the Ethic Committee of Cixi Hospital (Wenzhou, China; approval nos. 2008-005 and 2017-LS-25). Written informed consent was provided by all patients.

Patient consent for publication

Not applicable.

Competing interests

The authors declare that they have no competing interests.

References

- Chen C, Wu M, Zhang W, Lu W, Zhang M, Zhang Z, Zhang X and Yuan Z: MicroRNA-939 restricts Hepatitis B virus by targeting Jmjd3-mediated and C/EBP α -coordinated chromatin remodeling. *Sci Rep* 6: 35974, 2016.
- Chen W, Zheng R, Baade PD, Zhang S, Zeng H, Bray F, Jemal A, Yu XQ and He J: Cancer statistics in China, 2015. *CA Cancer J Clin* 66: 115-132, 2016.
- Zhang J, Gan L, Wu Z, Yan S, Liu X and Guo W: The influence of marital status on the stage at diagnosis, treatment, and survival of adult patients with gastric cancer: A population-based study. *Oncotarget* 8: 22385-22405, 2017.
- Yoo C, Ryu MH, Na YS, Ryoo BY, Lee CW and Kang YK: Vorinostat in combination with capecitabine plus cisplatin as a first-line chemotherapy for patients with metastatic or unresectable gastric cancer: Phase II study and biomarker analysis. *Br J Cancer* 114: 1185-1190, 2016.
- Padmanabhan N, Ushijima T and Tan P: How to stomach an epigenetic insult: The gastric cancer epigenome. *Nat Rev Gastroenterol Hepatol* 14: 467-478, 2017.
- Li Y, Liang J and Hou P: Hypermethylation in gastric cancer. *Clin Chim Acta* 448: 124-132, 2015.
- Zhang M and Du X: Noncoding RNAs in gastric cancer: Research progress and prospects. *World J Gastroenterol* 22: 6610-6618, 2016.
- Yang WY, Gu JL and Zhen TM: Recent advances of histone modification in gastric cancer. *J Cancer Res Ther* 10 (Suppl): 240-245, 2014.
- Sun DF, Zhang YJ, Tian XQ, Chen YX and Fang JY: Inhibition of mTOR signalling potentiates the effects of trichostatin A in human gastric cancer cell lines by promoting histone acetylation. *Cell Biol Int* 38: 50-63, 2014.
- Akiyama Y, Koda Y, Byeon SJ, Shimada S, Nishikawaji T, Sakamoto A, Chen Y, Kojima K, Kawano T, Eishi Y, *et al*: Reduced expression of SET7/9, a histone mono-methyltransferase, is associated with gastric cancer progression. *Oncotarget* 7: 3966-3983, 2016.
- Wang ZJ, Yang JL, Wang YP, Lou JY, Chen J, Liu C and Guo LD: Decreased histone H2B monoubiquitination in malignant gastric carcinoma. *World J Gastroenterol* 19: 8099-8107, 2013.
- Zhu X, Liu J, Xu X, Zhang C and Dai D: Genome-wide analysis of histone modifications by ChIP-chip to identify silenced genes in gastric cancer. *Oncol Rep* 33: 2567-2574, 2015.
- Sun M, Nie F, Wang Y, Zhang Z, Hou J, He D, Xie M, Xu L, De W, Wang Z, *et al*: lncRNA HOXA11-AS Promotes Proliferation and Invasion of Gastric Cancer by Scaffolding the Chromatin Modification Factors PRC2, LSD1, and DNMT1. *Cancer Res* 76: 6299-6310, 2016.
- Meng CF, Zhu XJ, Peng G and Dai DQ: Re-expression of methylation-induced tumor suppressor gene silencing is associated with the state of histone modification in gastric cancer cell lines. *World J Gastroenterol* 13: 6166-6171, 2007.
- Song IS, Ha GH, Kim JM, Jeong SY, Lee HC, Kim YS, Kim YJ, Kwon TK and Kim NS: Human ZNF312b oncogene is regulated by Sp1 binding to its promoter region through DNA demethylation and histone acetylation in gastric cancer. *Int J Cancer* 129: 2124-2133, 2011.
- Audia JE and Campbell RM: Histone Modifications and Cancer. *Cold Spring Harb Perspect Biol* 8: a019521, 2016.
- Perrigue PM, Najbauer J and Barciszewski J: Histone demethylase JMJD3 at the intersection of cellular senescence and cancer. *Biochim Biophys Acta* 1865: 237-244, 2016.
- Li Q, Hou L, Ding G, Li Y, Wang J, Qian B, Sun J and Wang Q: KDM6B induces epithelial-mesenchymal transition and enhances clear cell renal cell carcinoma metastasis through the activation of SLUG. *Int J Clin Exp Pathol* 8: 6334-6344, 2015.
- Xiang Y, Zhu Z, Han G, Lin H, Xu L and Chen CD: JMJD3 is a histone H3K27 demethylase. *Cell Res* 17: 850-857, 2007.
- Zhang Y, Shen L, Stupack DG, Bai N, Xun J, Ren G, Han J, Li L, Luo Y, Xiang R, *et al*: JMJD3 promotes survival of diffuse large B-cell lymphoma subtypes via distinct mechanisms. *Oncotarget* 7: 29387-29399, 2016.
- Bosman FT, Carneiro F, Hruban RH and Theise ND (eds): WHO Classification of Tumours of the Digestive System. Vol. 3, 4th edition. International Agency for Research on Cancer, Lyon, 2010.
- Otto T and Sicinski P: Cell cycle proteins as promising targets in cancer therapy. *Nat Rev Cancer* 17: 93-115, 2017.
- Shmakova A, Batie M, Druker J and Rocha S: Chromatin and oxygen sensing in the context of JmjC histone demethylases. *Biochem J* 462: 385-395, 2014.
- Chen S, Ma J, Wu F, Xiong LJ, Ma H, Xu W, Lv R, Li X, Villen J, Gygi SP, *et al*: The histone H3 Lys 27 demethylase JMJD3 regulates gene expression by impacting transcriptional elongation. *Genes Dev* 26: 1364-1375, 2012.
- Zhao W, Li Q, Ayers S, Gu Y, Shi Z, Zhu Q, Chen Y, Wang HY and Wang RF: Jmjd3 inhibits reprogramming by upregulating expression of INK4a/Arf and targeting PHF20 for ubiquitination. *Cell* 152: 1037-1050, 2013.
- Poreba E, Broniarczyk JK and Gozdzińska-Jozefiak A: Epigenetic mechanisms in virus-induced tumorigenesis. *Clin Epigenetics* 2: 233-247, 2011.
- Anderton JA, Bose S, Vockerodt M, Vrzalikova K, Wei W, Kuo M, Helin K, Christensen J, Rowe M, Murray PG, *et al*: The H3K27me3 demethylase, KDM6B, is induced by Epstein-Barr virus and over-expressed in Hodgkin's lymphoma. *Oncogene* 30: 2037-2043, 2011.
- Chen J: The Cell-Cycle Arrest and Apoptotic Functions of p53 in Tumor Initiation and Progression. *Cold Spring Harb Perspect Med* 6: a026104, 2016.
- Enyindah-Asonye G, Li Y, Xin W, Singer NG, Gupta N, Fung J and Lin F: CD6 Receptor Regulates Intestinal Ischemia/Reperfusion-induced Injury by Modulating Natural IgM-producing B1a Cell Self-renewal. *J Biol Chem* 292: 661-671, 2017.
- Li Y, Singer NG, Whitbred J, Bowen MA, Fox DA and Lin F: CD6 as a potential target for treating multiple sclerosis. *Proc Natl Acad Sci USA* 114: 2687-2692, 2017.
- Yan N, Xu L, Wu X, Zhang L, Fei X, Cao Y and Zhang F: GSKJ4, an H3K27me3 demethylase inhibitor, effectively suppresses the breast cancer stem cells. *Exp Cell Res* 359: 405-414, 2017.
- Sedrak H, El-Garem N, Naguib M, El-Zawahry H, Esmat M and Rashed L: Vascular endothelial growth factor before and after locoregional treatment and its relation to treatment response in hepatocellular carcinoma patients. *Asian Pacific Journal of Tropical Biomedicine* 5: 1005-1009, 2015.
- Ha SD, Cho W and Kim SO: HDAC8 Prevents Anthrax Lethal Toxin-induced Cell Cycle Arrest through Silencing PTEN in Human Monocytic THP-1 Cells. *Toxins (Basel)* 9: E162, 2017.

34. Kennedy R and Klein U: Aberrant Activation of NF- κ B Signalling in Aggressive Lymphoid Malignancies. *Cells* 7: E189, 2018.
35. Staudt LM: Oncogenic activation of NF-kappaB. *Cold Spring Harb Perspect Biol* 2: a000109, 2010.
36. Tang B, Qi G, Tang F, Yuan S, Wang Z, Liang X, Li B, Yu S, Liu J, Huang Q, *et al*: Aberrant JMJD3 Expression Upregulates Slug to Promote Migration, Invasion, and Stem Cell-Like Behaviors in Hepatocellular Carcinoma. *Cancer Res* 76: 6520-6532, 2016.
37. Yin X, Yang S, Zhang M and Yue Y: The role and prospect of JMJD3 in stem cells and cancer. *Biomed Pharmacother* 118: 109384, 2019.
38. Aguirre-Gamboa R, Gomez-Rueda H, Martínez-Ledesma E, Martínez-Torteya A, Chacolla-Huaringa R, Rodríguez-Barrientos A, Tamez-Peña JG and Treviño V: SurvExpress: An online biomarker validation tool and database for cancer gene expression data using survival analysis. *PLoS One* 8: e74250, 2013.
39. Goswami CP and Nakshatri H: PROGgeneV2: Enhancements on the existing database. *BMC Cancer* 14: 970, 2014.
40. Goldman M, Craft B, Swatloski T, Cline M, Morozova O, Diekhans M, Haussler D and Zhu J: The UCSC Cancer Genomics Browser: Update 2015. *Nucleic Acids Res* 43D: D812-D817, 2015.
41. Tang Z, Li C, Kang B, Gao G, Li C and Zhang Z: GEPIA: A web server for cancer and normal gene expression profiling and interactive analyses. *Nucleic Acids Res* 45W: W98-W102, 2017.
42. Chandrashekar DS, Bashel B, Balasubramanya SAH, Creighton CJ, Ponce-Rodriguez I, Chakravarthi B VSK and Varambally S: UALCAN: A Portal for Facilitating Tumor Subgroup Gene Expression and Survival Analyses. *Neoplasia* 19: 649-658, 2017.
43. Vasaikar SV, Straub P, Wang J and Zhang B: LinkedOmics: Analyzing multi-omics data within and across 32 cancer types. *Nucleic Acids Res* 46D: D956-D963, 2018.
44. Cerami E, Gao J, Dogrusoz U, Gross BE, Sumer SO, Aksoy BA, Jacobsen A, Byrne CJ, Heuer ML, Larsson E, *et al*: The cBio cancer genomics portal: An open platform for exploring multi-dimensional cancer genomics data. *Cancer Discov* 2: 401-404, 2012.
45. Rhodes DR, Yu J, Shanker K, Deshpande N, Varambally R, Ghosh D, Barrette T, Pandey A and Chinnaiyan AM: ONCOMINE: A cancer microarray database and integrated data-mining platform. *Neoplasia* 6: 1-6, 2004.



This work is licensed under a Creative Commons Attribution-NonCommercial-NoDerivatives 4.0 International (CC BY-NC-ND 4.0) License.